Long-Term Liraglutide Administration Induces Pancreas Neogenesis in Adult T2DM Mice

Hongjun Deng[1], Fengying Yang[1], Xiaoyi Ma[1], Ying Wang[1], Qi Chen[1], and Li Yuan[1] 🄳

Abstract

In vivo beta-cell neogenesis may be one way to treat diabetes. We aimed to investigate the effect of glucagon-like peptide-1 (GLP-1) on beta-cell neogenesis in type 2 diabetes mellitus (T2DM). Male C57BL/6J mice, 6 wk old, were randomly divided into three groups: Control, T2DM, and T2DM + Lira. T2DM was induced using high-fat diet and intraperitoneal injection of streptozotocin (40 mg/kg/d for 3 d). At 8 wk after streptozotocin injection, T2DM + Lira group was injected intraperitoneally with GLP-1 analog liraglutide (0.8 mg/kg/d) for 4 wk. Apparently for the first time, we report the appearance of a primitive bud connected to pancreas in all adult mice from each group. The primitive bud was characterized by scattered single mono-hormonal cells expressing insulin, GLP-1, somatostatin, or pancreatic polypeptide, and four-hormonal cells, but no acinar cells and ductal epithelial cells. Monohormonal cells in it were small, newborn, immature cells that rapidly proliferated and expressed cell markers indicative of immaturity. In parallel, Ngn3+ endocrine progenitors and Nestin+ cells existed in the primitive bud. Liraglutide facilitated neogenesis and rapid growth of acinar cells, pancreatic ducts, and blood vessels in the primitive bud. Meanwhile, scattered hormonal cells aggregated into cell clusters and grew into larger islets; polyhormonal cells differentiated into monohormonal cells. Extensive growth of exocrine and endocrine glands resulted in the neogenesis of immature pancreatic lobes in adult mice of T2DM + Lira group. Contrary to predominant acinar cells in mature pancreatic lobes, there were still a substantial number of mesenchymal cells around acinar cells in immature pancreatic lobes, which resulted in the loose appearance. Our results suggest that adult mice preserve the capacity of pancreatic neogenesis from the primitive bud, which liraglutide facilitates in adult T2DM mice. To our knowledge, this is the first time such a phenomenon has been reported.

Keywords

T2DM, GLP-1, pancreatic stem cell, pancreas neogenesis

Introduction

Loss of functional beta-cell mass is a common pathogenic characteristic of type 2 diabetes mellitus (T2DM). Thus, restoration of functional beta-cell mass is the major goal of diabetes treatment. Although the existence of adult pancreatic stem cells remains controversial, numerous studies have suggested that, in adulthood, new endocrine cells form by differentiation of duct cells, which bud to generate new islets to serve future metabolic needs[1]. Single and clustered beta-cells adjacent to ducts are seen as sites of beta-cell neogenesis[2]. These findings raise the possibility that facilitating beta-cell neogenesis in adult pancreas may be a novel strategy for in vivo restoration of beta-cell mass in diabetes treatment.

Glucagon-like peptide-1 (GLP-1) is a peptide hormone and member of the incretin family[3,4]. It stimulates insulin secretion, suppresses glucagon release, and decreases gastric emptying[4]. Studies in mice and humans have shown anti-inflammatory effects, improved lipid metabolism and hepatic steatosis, and weight loss with GLP-1 receptor (GLP-1R)

[1] Department of Endocrinology, Union Hospital, Tongji Medical College, Huazhong University of Science and Technology, Wuhan, Hubei, P.R. China

Corresponding Author:
Li Yuan, Department of Endocrinology, Union Hospital, Tongji Medical College, Huazhong University of Science and Technology, 1277 Jiefang Avenue, Wuhan, Hubei 430022, P.R. China.
Email: yuanli18cn@126.com

agonists[5–7]. In addition, GLP-1 increases pancreatic beta-cell gene expression, promotes beta-cell proliferation, and inhibits apoptosis[8,9]. In recent years, GLP-1 has attracted considerable attention for its effects on beta-cell growth and differentiation[10,11]. One study reported that GLP-1R (GPR119) activation increases beta-cell mass by stimulating beta-cell neogenesis in the pancreatic duct[12]. Other studies reported that activation of GLP-1 signaling induces reprogramming of pancreatic exocrine cells or alpha-cells into beta-cells in mice[13,14]. These findings suggest a possible role of GLP-1 in promoting beta-cell neogenesis in vivo.

Moreover, in addition to beta-cells, exocrine cells may also be affected by GLP-1. Quantitative histology studies showed that treatment with the GLP-1 analog liraglutide increased exocrine cell mass in at least three species, including mice, rats, and nonhuman primates, with normal composition of endocrine and exocrine cellular compartments[15]. Pharmacological GLP-1R activation increases pancreatic mass independent of changes in deoxyribonucleic acid content or cell proliferation in mice[16]. These findings in different species provide hope that GLP-1 analog treatment may promote both beta-cell and exocrine cell neogenesis, but whether these effects occur in the context of T2DM remains unclear. To address this question, we administered the GLP-1 analog liraglutide for 4 wk to mice with a T2DM-like phenotype induced by a high-fat diet and streptozotocin injection[17]. Liraglutide has long half-life in vivo, which allowed us to examine the in vivo effects of GLP-1[18].

However, despite all the beneficial effects of GLP-1, it should be noted that GLP-1 mimetic therapy may accelerate the development of pancreatic intraepithelial neoplasia and exacerbate chronic pancreatitis[19,20]. Although some studies have found no evidence of an association between GLP-1R agonist exenatide and pancreatitis[21], other reports describe an increased incidence of acute pancreatitis in humans treated with exenatide[22]. As pancreatitis and pancreatic cancer are more common in T2DM patients[23,24], GLP-1 analogs may further increase the risk of these diseases in the context of T2DM. For these reasons, histological changes in pancreas of T2DM mice were also explored after liraglutide treatment.

Materials and Methods

Animals

C57BL/6J mice (4 wk old) were obtained from the Laboratory Animal Center of Hubei Province, China [quality certification number: SYXK (E) 2016-0057]. Male and female C57BL/6J mice, 8 wk old, were crossed to produce offspring. Animals were housed in the specific pathogen-free mouse room in the Laboratory Animal Center (Tongji Medical College, Wuhan, Hubei Province, China). All of the experimental procedures involving animals were conducted in accordance with the Institutional Animal Care Guidelines of Huazhong University of Science and Technology, China,

and were approved by the Experimental Animal Committee of Huazhong University of Science and Technology, Hubei Province, China.

Study Design

Six-week-old male mice with random blood glucose levels of 6 to 10 mmol/l were randomly divided into three groups ($n = 8$ in each group): (1) Control, (2) T2DM, and (3) T2DM + Lira. The Control group was fed with regular chow, while the other groups were fed with a high-fat diet (Research Diets, New Brunswick, NJ, USA) containing 60 kcal% fat throughout the study. After 4 wk, mice of T2DM and T2DM + Lira groups were injected intraperitoneally with streptozotocin once daily for 3 d (Sigma-Aldrich, St Louis, MO, USA; 40 mg/kg/d). T2DM model creation was considered successful in mice with random blood glucose level >16.7 mmol/l[17]. All 16 mice in T2DM and T2DM + Lira groups met the criterion for successful T2DM model development.

At 8 wk after streptozotocin injection, mice of T2DM + Lira group were intraperitoneally injected with liraglutide (Novo Nordisk A/S, Bagsvaerd, Denmark; 0.8 mg/kg/d) daily for 4 wk, while mice of Control and T2DM groups received daily injections of 0.5 ml of sterile saline. Body weight was measured weekly.

Intraperitoneal insulin tolerance tests (IPITTs) and intraperitoneal glucose tolerance tests (IPGTTs) were performed in all mice of the three groups before sacrifice. Serum insulin and glucagon concentrations were determined by ELISA kits (ALPCO, Salem, NH, USA; EZGLU-30K, Millipore, Boston, MA, USA). Intact pancreatic tissue removed from mice was used for hematoxylin–eosin (HE) staining, immunohistochemistry (IHC), immunofluorescence (IF), or reverse transcription-polymerase chain reaction (RT-PCR) analysis.

Mature and immature pancreatic lobes in pancreatic sections from T2DM + Lira mice were compared by HE staining, IHC, and IF.

Day 16 embryos ($n = 8$) were removed from euthanized pregnant mice under sterile conditions. Embryonic pancreas (E 16d) was removed from these embryos and subjected to HE staining and IF. Immature pancreatic lobes and embryonic pancreases were compared by HE staining and IF.

Blood Glucose Levels Measurement, IPITTs, and IPGTTs

Blood glucose levels were measured using OneTouch blood glucose meter (LifeScan, Burnaby, Canada). Blood was collected via tail vein. For IPITTs, animals fasted for 6 h and were then intraperitoneally injected with insulin (0.75 IU/kg). For IPGTTs, mice fasted for 16 h and were injected intraperitoneally with glucose (2 g/kg). Blood glucose levels were measured at 0, 15, 30, 60, and 90 min after insulin or glucose injection using OneTouch blood glucose meter (LifeScan).

Insulin, Glucagon Concentrations Measurements, and RT-PCR Analysis

After mice had fasted for 16 h, insulin and glucagon concentrations in serum were determined using ELISA kits (ALPCO; EZGLU-30K) according to the manufacturer's protocols. Total ribonucleic acid (RNA) from pancreatic tissue was extracted using TRIzol reagent (Takara Shuzo Co., Ltd, Kyoto, Japan). Experiments were performed in triplicate. The relative transcript level of insulin was normalized to glyceraldehyde-3-phosphate dehydrogenase (GAPDH) and calculated using the $2^{-\Delta\Delta CT}$ statistical method. The primers used were as follows:
InsulinForward: 5′-CTGGTGCAGCACTGATCTACA-3′

Reverse: 5′-AGCGTGGCTTCTTCTACACAC-3′
GAPDHForward: 5′-CATGGCCTTCCGTGTTC-CTA-3′
Reverse: 5′-CCTGCTTCACCACCTTCTTGAT-3′

Hematoxylin–Eosin Staining and Immunohistochemistry

After the mice were sacrificed, pancreatic tissues were harvested, fixed in 4% paraformaldehyde (Sigma-Aldrich), embedded in paraffin blocks (Sigma-Aldrich), sectioned (5 μm), and used for HE staining and IHC analysis. HE and IHC were performed as previously described[25]. For immunohistochemical staining, pancreatic sections were stained with primary antibodies against amylase (Boster Biological Technology, Wuhan, Hubei Province, China) and cytokeratin 19 (CK19) (Servicebio, Wuhan, Hubei Province, China). Horseradish peroxidase-conjugated goat antirabbit immunoglobulin G (H+L) (IgG (H + L)) (Servicebio) was used as secondary antibody.

Immunofluorescence Staining

IF staining was performed as previously described[25]. The following primary antibodies were used: guinea pig anti-insulin and rabbit anti-insulin (ab7842 and ab63820; Abcam, Cambridge, UK), rabbit antiglucagon and sheep antiglucagon (ab92517 and ab36232; Abcam), rabbit anti-GLP1 and mouse anti-GLP1 (ab22625 and ab23472; Abcam), mouse anti-GLP1R (sc390773; Santa Cruz, Dallas, TX, USA), rabbit anti-GLP1R (NBP1-97308; Novus, CO, USA), mouse antisomatostatin (sc-74556; Santa Cruz), goat antipancreatic polypeptide (Ab77192; Abcam), rabbit anti-Ki67 (ARG53222; Arigo, Taiwan, China), rabbit anti-pancreatic and duodenal homeobox 1 (PDX1) (ab47267; Abcam), rabbit anti-NK6 homeobox transcription factor-related locus 1 (NKX6.1) (NBP1-49672SS; Novus), rabbit anti-forkhead box O1A (FoxO1A) (ab39670; Abcam), rabbit anti-octamer-binding transcrition factor-4 (OCT4) (GTX101497; GeneTex, CA, USA), rabbit anti-neurogenin3 (Ngn3) (2325032; Millipore, Boston, MA, USA), and mouse anti-Nestin (GTX630201; GeneTex). Detection was performed using secondary antibodies conjugated to Alexa488 (ab150185 and ab150077; Abcam), Alexa594 (ab150088, ab150132, ab150116 and ab150180; Abcam), or Alexa647 (ab150115; Abcam) fluorescent dye. 4'6'-diamidino-2-phenyl-indole (DAPI) (Invitrogen, Carlsbad, CA, USA) was used for nuclear staining.

Equipment and Settings

For HE and IHC analysis, pancreatic sections were observed with a light microscope (LIOO S600T, China) and images were captured using a computer image analysis system (Caseviewer2.0, 3D HISTECH, Hungary). For IF analysis, images were acquired using a confocal microscope (C-1/TE200U; Nikon, Tokyo, Japan). The numerical aperture for the confocal microscope was 0.75, and the width of the optical slice was 635 μm. All statistical graphs were made with GraphPad Prism (version 7.0; CA, USA). All images were processed in Adobe Photoshop CS6 (version 13.0; Adobe Systems, Mountain View, CA, USA).

Statistical Analyses

Results were expressed as mean $\pm$ SD. Data were analyzed using one-way analysis of variance (ANOVA) followed by the Bonferroni post hoc test. For experiments with multiple variables, two-way ANOVA was used. A value of $P < 0.05$ was considered significant.

Results

Liraglutide Administration Induces Intact Pancreas Neogenesis from the Primitive Bud

The T2DM group showed beta-cell failure that was partially restored by liraglutide, as shown by the IPITTs and IPGTTs, as well as increased fasting insulin concentration and insulin messenger-RNA expression (Fig. 1A, B, D,E). These results indicate that liraglutide induces diabetes remission partially by restoring beta-cell function. Liraglutide treatment also induced weight loss in T2DM mice and suppressed glucagon secretion (Fig. 1C, F).

Light microscopy analysis of pancreas tissue revealed a novel structure with a loose cellular morphology, which we termed "tubuli-vesicular structure." To our knowledge, this structure has not been reported previously. The novel structure was identified in all mouse groups (Figs. 1G, 2A). Upon further investigation, we detected scattered single insulin$^+$ cells, GLP-1$^+$ cells, and insulin$^+$/GLP-1$^+$ bihormonal cells (indicated by white arrows), suggesting the presence of hormone-producing endocrine cells. However, these endocrine cells were different from those in the pancreas: bihormonal cells and alpha-cells in the tubuli-vesicular structure produced much more GLP-1 than glucagon (see supplementary Fig. S1). To confirm this result, glucagon and GLP-1 expressions were detected using two sets of antibodies, and the results were consistent. Furthermore, the majority of
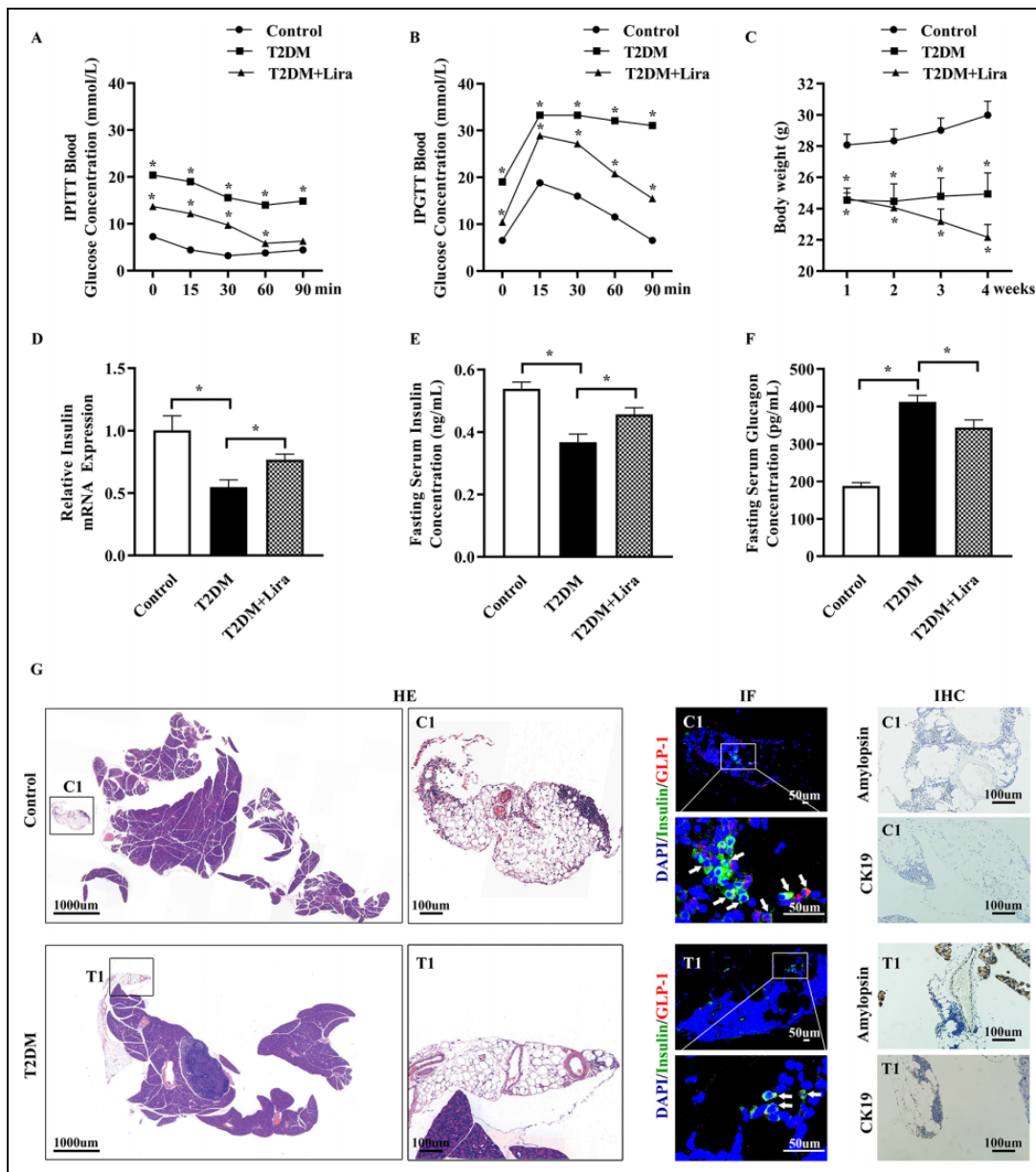
Figure 1. A tubuli-vesicular structure connected to pancreas in adult mice. (A and B) Line graphs show five measurements of blood glucose concentration in the IPITT and IPGTT tests in the Control group (dots), T2DM group (squares), and T2DM + Lira group (triangles; $n = 8$ mice per group). (C) Mean body weight of mice in Control group (dots), T2DM group (squares), and T2DM + Lira group (triangles; $n = 8$ mice per group) measured once a week during sterile saline or liraglutide intervention. (D) Bar graph indicates RT-PCR analysis of insulin gene expression in pancreatic tissue samples from the Control group (white bar), T2DM group (black bar), and T2DM + Lira group (hatched bar; $n = 4$ mice per group). (E and F) Bar graphs indicate fasting serum insulin concentration and fasting serum glucagon concentration in the Control group (white bar), T2DM group (black bar), and T2DM + Lira group (dotted bar; $n = 8$ mice per group). (G) Hematoxylin–eosin (HE) images show representative photoscans of pancreatic sections from Control and T2DM groups. C1 and T1 images on the right are enlarged views of the photoscans which show the tubuli-vesicular structure connected to pancreas. Confocal images show double immuno-fluorescence (IF) staining for insulin (green) and GLP-1 (red) on the corresponding pancreatic sections of the HE images. White arrows indicate cells coexpressing insulin and GLP-1 in the tubuli-vesicular structure. Immunohistochemistry (IHC) images show IHC staining for amylopsin and CK19 on pancreatic sections from Control and T2DM groups; no immunoreactive cells (brown cells) were found in the tubuli-vesicular structure. Data were analyzed using two-way analysis of variance. Significant differences: *$P < 0.05$. CK19: cytokeratin 19; DAPI: 4'6'-diamidino-2-phenyl-indole; GLP-1: glucagon-like peptide-1; IPITT: intraperitoneal insulin tolerance test; IPGTT: intraperitoneal glucose tolerance test; Lira: liraglutide; mRNA: messenger ribonucleic acid; RT-PCR: reverse transcription-polymerase chain reaction; T2DM: type 2 diabetes mellitus.
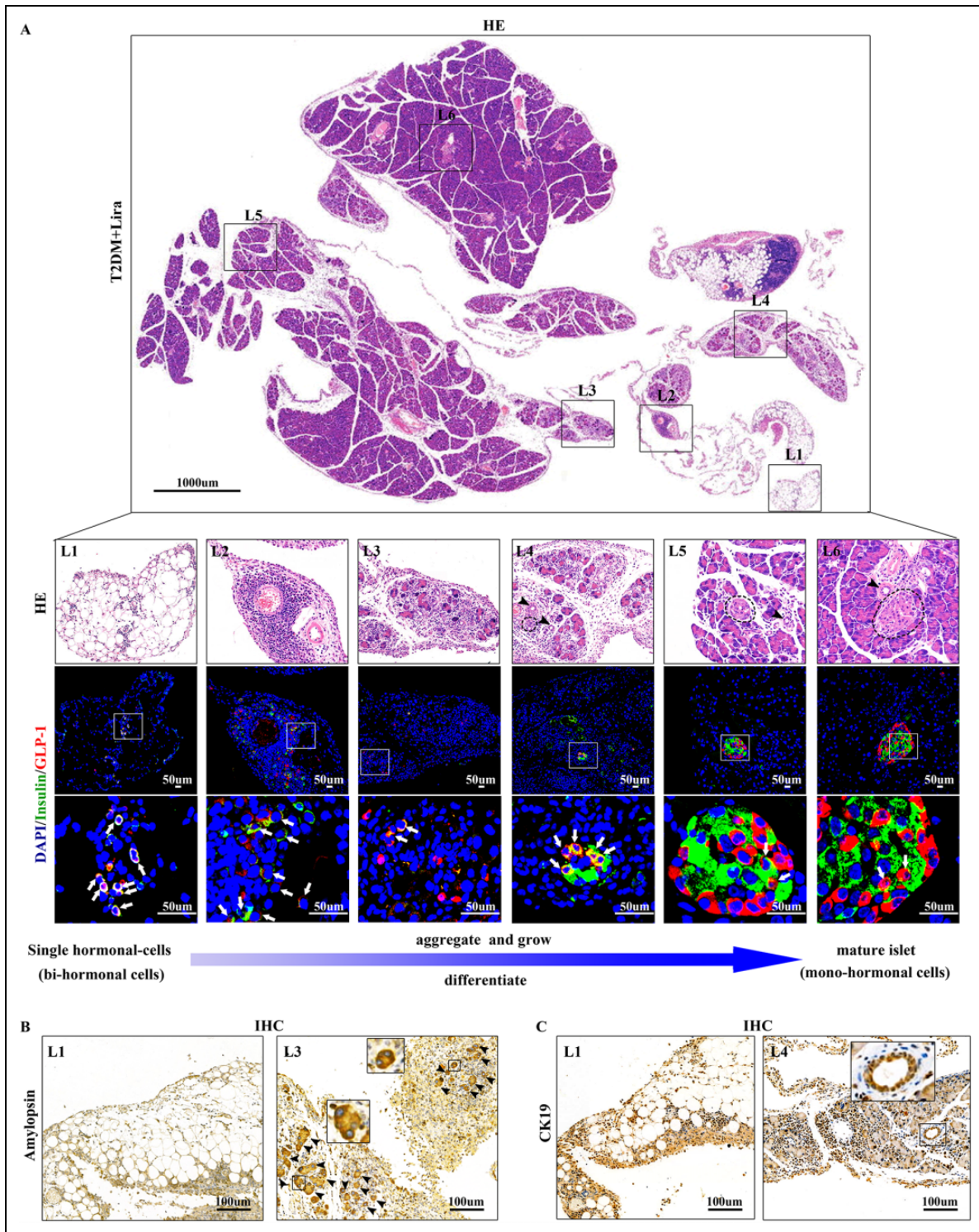
Figure 2. Liraglutide administration induces intact pancreas neogenesis in adult T2DM mice. (A) Hematoxylin–eosin (HE) images show representative photoscans of pancreatic sections from T2DM + Lira group. L1 to L6 images are enlarged views of the photoscans above. Confocal images show double immunofluorescence (IF) staining for insulin (green) and GLP-1 (red) on the corresponding pancreatic sections of the HE images. White arrows indicate cells coexpressing insulin and GLP-1. L1 to L5 images show five stages of neogenic pancreas. L6 image shows mature pancreatic lobes. Black arrows in L4-L6 indicate pancreatic ducts. Dotted circles in L4-L6 indicate islet-like cell clusters and islets. (B) Immunohistochemistry (IHC) images show IHC staining for amylopsin on pancreatic sections from T2DM + GLP-1 group. Amylopsin-immunoreactive cells were not found in stage L1, but they began to be detectable in stage L3 (brown cells, indicated by black arrowheads). Insets show enlarged views of amylopsin-immunoreactive acinar cells in neogenic pancreas. (C) IHC images show IHC staining for CK19 on pancreatic sections from T2DM + GLP-1 group. CK19-immunoreactive cells were not found in stage L1, but they began to be detectable in stage L4 (brown cells). Insets show enlarged views of CK19-immunoreactive pancreatic duct in neogenic pancreas. CK19: cytokeratin 19; DAPI: 4'6'-diamidino-2-phenyl-indole; GLP-1: glucagon-like peptide-1; Lira: liraglutide; T2DM: type 2 diabetes mellitus.

endocrine cells were incompletely differentiated insulin$^+$/GLP-1$^+$ bihormonal cells rather than insulin$^+$ cells or GLP-1$^+$ cells (59.38% $\pm$ 3.1% vs. 21.17% $\pm$ 5.42% and 19.44% $\pm$ 1.94%; 8 mice, one pancreatic section per mouse). Additionally, contrary to endocrine cells aggregating into islets in pancreas, single hormonal cells were scattered throughout the tubuli-vesicular structure.

We failed to detect the acinar cell marker amylase or ductal epithelial cell marker CK19 in the tubuli-vesicular structure by IHC, implying that this structure differs from mature adult mouse pancreas (Fig. 1G). Therefore, we speculate that the tubuli-vesicular structure is a pancreatic tissue in a more primitive state. Consistent with this idea, liraglutide induced neogenesis of intact pancreatic lobes, complete with exocrine and endocrine glands, from the tubuli-vesicular structure (Fig. 2A).

Based on the range of tissues that we observed across the three mouse groups, we divided the pancreas neogenesis process into five stages (L1–L5) based on unique, chronologically related characteristics of exocrine and endocrine glands, with L6 representing the mature pancreatic lobe in adult mice and serving as a control. Stage L1 was the tubuli-vesicular structure. More mesenchymal and endocrine cells were present in stage L2 than in stage L1. Then, acinar cells and pancreatic ducts (indicated by black arrowheads in IHC and HE images) were generated, which resulted in the formation of the preliminary shape of pancreatic lobes (stage L3–L4; Fig. 2A–C). GLP-1$^+$ alpha-cells began to express glucagon in stage L3 (see supplementary Fig. S1). With extensive growth of acinar cells and rapid decrease in mesenchymal cells, neogenic pancreatic lobes gradually lost their loose appearance. Single hormonal cells aggregated and formed islet-like clusters of fewer than 10 cells, which fused and/or grew into larger aggregates before the bihormonal cells differentiated into monohormonal cells (stage L4–L5). Extensive growth of exocrine and endocrine cells resulted in the neogenesis and gradual maturation of immature pancreatic lobes (stages L3–L5) in adult T2DM + Lira mice (Fig. 2A). No histological abnormalities, such as pancreatic cancer, were observed in immature pancreatic lobes (Fig. 2A).

Each stage was defined as follows:

1) Stage L1. The tubuli-vesicular structure contained scattered cells positive for insulin and/or GLP-1 but no exocrine cells. Alpha-cells mainly produced GLP-1 instead of glucagon.
2) Stage L2. The number of mesenchymal and hormonal cells increased, and exocrine cells remained absent.
3) Stage L3. Immature pancreatic lobes formed with scattered polyhormonal cells. Acinar cells of different sizes and shapes were generated for the first time. Alpha-cells started to express glucagon. Immature pancreatic lobes with a loose appearance began to take shape.
4) Stage L4. Immature pancreatic lobes formed with immature polyhormonal islets. Pancreatic ducts started to form, accompanied by the rapid decrease in mesenchymal cells. This stage was characterized by the formation of islet-like clusters (<10 cells), but a substantial number of mesenchymal cells remained accumulated around acinar cells, resulting in the loose appearance.
5) Stage L5. Immature pancreatic lobes showed the formation of monohormonal (insulin) core islets. The extensive growth of acinar cell numbers evoked the gradual loss of the loose appearance of the immature pancreatic lobes. Islet-like cell clusters fused and/or grew into larger aggregates, with prominent differentiation from bihormonal to monohormonal cells.

As demonstrated above, stages L3–L5 were defined as immature pancreatic lobes, which had the preliminary shape of pancreatic lobe but contained immature endocrine and exocrine glands in comparison with mature pancreatic lobe (L6). The major differences were as follows. In the endocrine gland of mature pancreatic lobe, alpha-, beta-, δ- and pancreatic polypeptide (PP)-cells aggregated into large islets with monohormonal insulin core. However, immature pancreatic lobes contained scattered single endocrine cells or islet-like clusters of fewer than 10 cells, and these clusters grew larger into islets with immature polyhormonal cells (Fig. 3A). The proportion of incompletely differentiated insulin$^+$/GLP-1$^+$ bihormonal cells among total endocrine cells was much higher in immature pancreatic lobes than in mature pancreatic lobes (L3, L4, L5 vs. L6: 0.419 $\pm$ 0.039, 0.387 $\pm$ 0.035, 0.095 $\pm$ 0.017 vs. 0.03 $\pm$ 0.001, respectively; 8 mice, one pancreatic section per mouse; Fig. 3B).

Exocrine gland in mature pancreatic lobe was dominated by exocrine cells with nearly no mesenchymal cells around acinar cells. However, in immature pancreatic lobes, there were a substantial number of mesenchymal cells around acinar cells. The loose appearance of immature pancreatic lobes was similar to that of the embryonic pancreas (Fig. 3C).

In mice, embryonic pancreas is described as immature pancreas[26]. During development, embryonic pancreas loses its loose appearance in the first week after birth and develops the packed appearance as seen in the adult[26]. New pancreatic lobes are not generated in mice older than 4 wk; thus, immature pancreatic lobes with a loose appearance do not exist in mice older than 4 wk[26]. Accordingly, pancreatic neogenesis is defined as the generation of immature pancreatic lobes in mice older than 4 wk.

Immature pancreatic lobes (stages L3–L5) were not observed in the Control or T2DM groups but were identified in all mice of T2DM + Lira group, implying that these lobes correspond to neogenic pancreas (Fig. 4A–C). This result led to the conclusion that liraglutide treatment, rather than beta-cell damage during diabetes pathogenesis, induces intact pancreas neogenesis. Based on the continuous process of
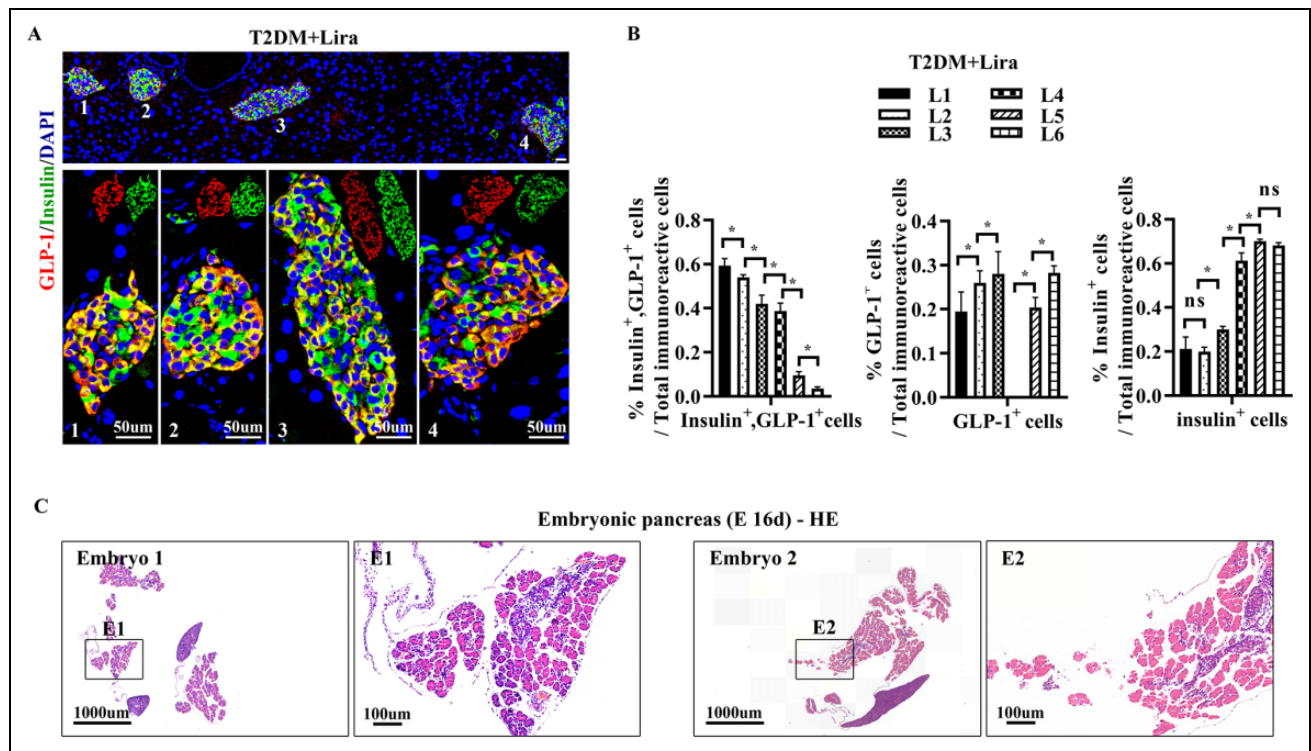
Figure 3. Endocrine cell characteristics in neogenic pancreas of T2DM + Lira mice. (A) Representative images of pancreatic sections from the T2DM + Lira group double immunostaining for insulin (green) and GLP-1 (red). Cells positive for both insulin and GLP-1 appear yellow. All GLP-1$^+$ cells in islets (numbers 1 to 4) of neogenic pancreas coexpressed insulin and appeared yellow. (B) Bar graphs show ratios of insulin$^+$/GLP-1$^+$ bi-hormonal cells or insulin$^+$ cells or GLP-1$^+$ cells to immunoreactive cells in five stages of neogenic pancreas of T2DM + Lira group (eight mice, one pancreatic section per mice). (C) HE images show representative photoscans of pancreatic sections from 16-d mice embryos. E1, E2 on the right are enlarged views of the HE photoscans on the left. Data were analyzed using one-way ANOVA. Significant differences: *$P < 0.05$. ns indicates nonsignificance. CK19: cytokeratin 19; DAPI: 4'6'-diamidino-2-phenyl-indole; GLP-1: glucagon-like peptide-1; HE: hematoxylin–eosin; Lira: liraglutide; T2DM: type 2 diabetes mellitus.

neogenic pancreas development, we conclude that the tubuli-vesicular structure is the primitive bud that gives rise to immature pancreatic lobes.

Scattered single insulin$^+$ cells, islet-like cell clusters, and islets in neogenic pancreas increased total beta-cell mass in T2DM + Lira mice, which may help explain the recovery of beta-cell function. In parallel, liraglutide treatment promoted angiogenesis in neogenic pancreas, which ensured the supply of nutrients needed for growth (see supplementary Fig. S1).

Scattered Single Alpha- and Beta-Cells in Neogenic Pancreas Are Newborn Immature Cells

Scattered single alpha- and beta-cells were present in the neogenic pancreas at stages L1–L3 (Fig. 2A) and were considered to be newborn immature endocrine cells because of their round shape and small size, in contrast to the more abundant polygonal mature beta-cells; and also because of their rapid proliferation, in contrast to the slow turnover of mature beta- and alpha-cells (Fig. 5A, B)[27,28].

To exclude the possibility that the single beta-cells were mature, we confirmed their identity using confocal microscopy. The mature beta-cell markers FoxO1 and NKX6.1 showed low expression in neogenic beta-cells (indicated by white arrows; Fig. 5C). PDX1 was highly expressed in neogenic beta-cells. In contrast to the nuclear localization of NKX6.1 and PDX1 in mature beta-cells, these proteins were mainly localized in the cytoplasm of neogenic beta-cells, which may restrict their binding to insulin gene promoter to stimulate transcription[29]. The low expression levels and cytoplasmic localization of mature beta-cell transcription factors suggest that single beta-cells are immature.

To exclude the possibility that the single alpha-cells were mature, we took advantage of the fact that during development, immature alpha-cells express prohormone convertase 1/3 (PC1/3), PC2, and GLP-1 in addition to glucagon, while mature alpha-cells mainly produce glucagon and only trace amounts of GLP-1[30,31]. Surprisingly, alpha-cells in the neogenic pancreas at stage L1–L2 mainly expressed GLP-1, whereas glucagon immunoreactivity was hardly detectable (Fig. 5D). Consistent with
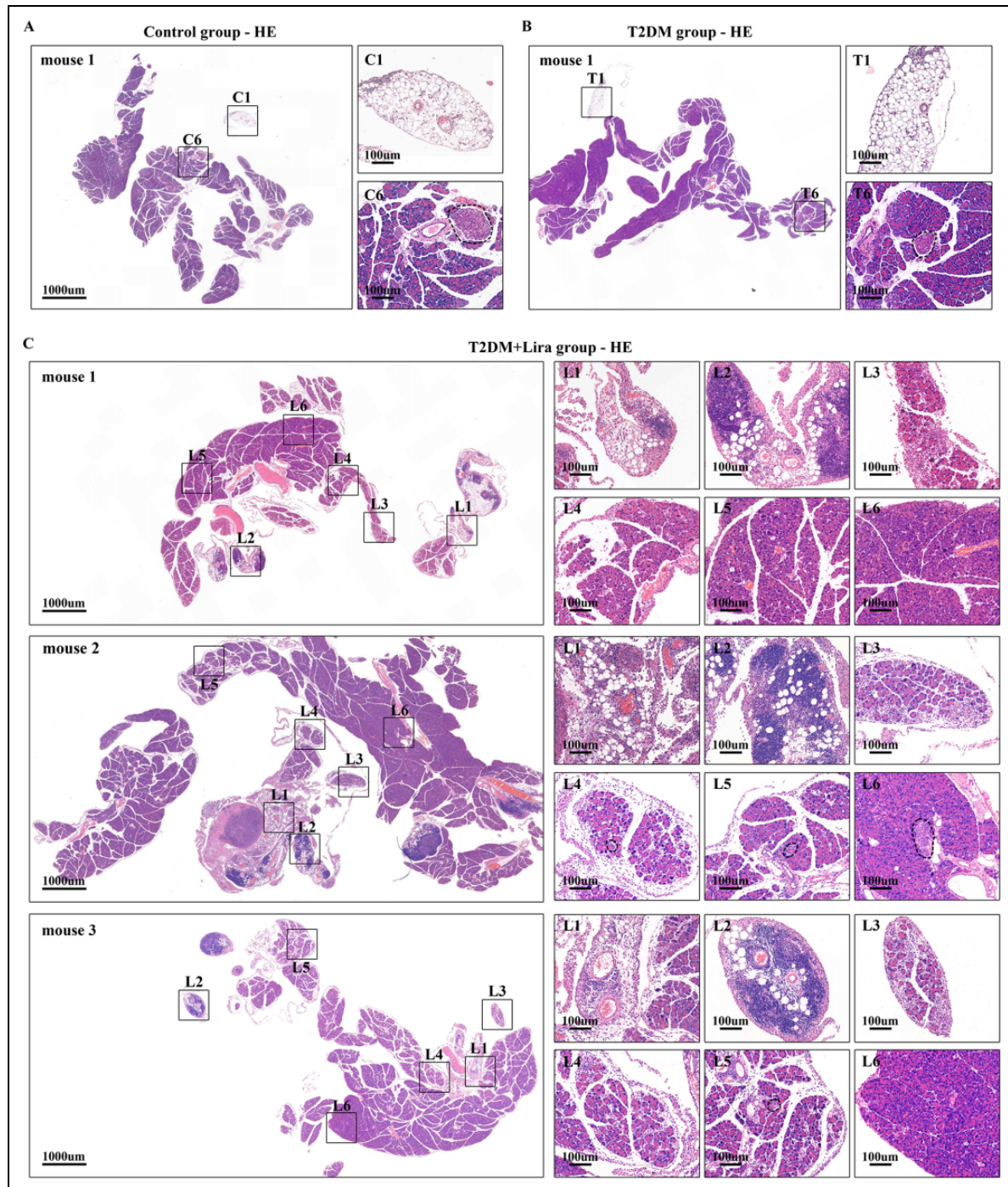
Figure 4. Pancreas neogenesis does not occur in T2DM group. (A and B) HE images show representative photoscans of pancreatic sections from Control and T2DM groups. C1 and T1 images on the right are enlarged views of the tubuli-vesicular structure in the HE photoscans on the left. C6 and T6 images on the right are enlarged views of mature pancreatic lobes in the HE photoscans on the left. (C) HE images show representative photoscans of pancreatic sections from T2DM + Lira group. L1–L5 images on the right are enlarged views of neogenic pancreas. L6 image on the right is enlarged view of mature pancreatic lobes. Dotted circles indicate islet-like cell clusters and islets. HE: hematoxylin–eosin; Lira: liraglutide; T2DM: type 2 diabetes mellitus.

this result, PC1/3 was highly expressed in the identified alpha-cells, whereas PC2 expression was extremely low (Fig. 5D). These results indicate that alpha-cells in neogenic pancreas at stage L1–L2 were immature. However, as demonstrated earlier (see supplementary Fig. S1), single alpha-cells in immature pancreatic lobes (stage L3) expressed glucagon, reflecting gradual maturation of alpha-cells induced by liraglutide.
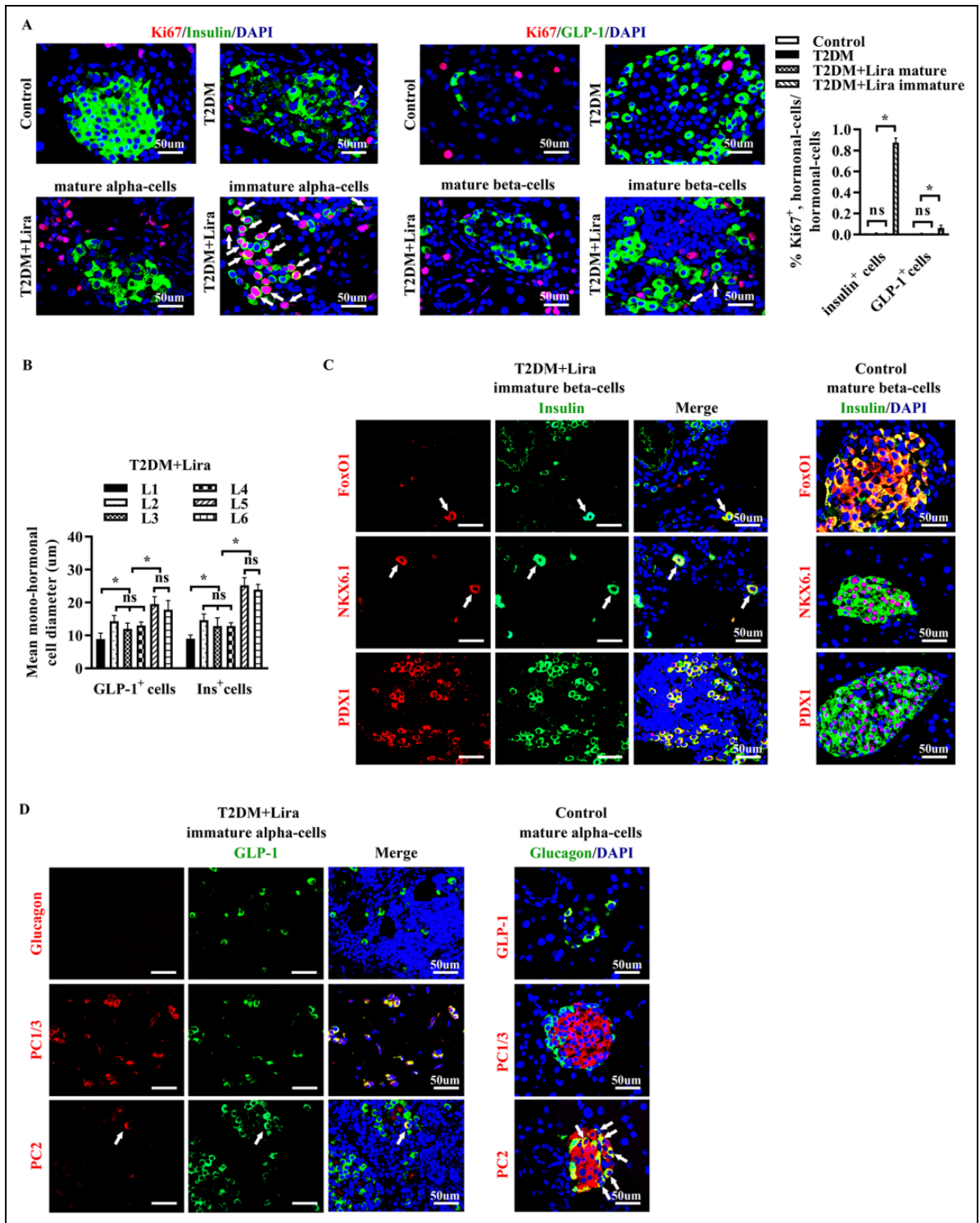
Figure 5. Newborn immature beta- and alpha-cells in neogenic pancreas. (A) Representative images of pancreatic sections from Control, T2DM, and T2DM + Lira groups after double immunostaining for Ki67 (red) and insulin or GLP-1 (green). Ki67$^+$/insulin$^+$ beta-cells and Ki67$^+$/GLP-1$^+$ alpha-cells are indicated with white arrows. The bar graph on the left shows the percentage of Ki67$^+$/insulin$^+$ cells among all insulin$^+$ cells. The bar graph on the right shows the percentage of Ki67$^+$/GLP-1$^+$ cells among all GLP-1$^+$ cells ($n = 4$ mice per group, five pancreatic sections per mouse). Data were analyzed using two-way ANOVA. (B) The bar graph shows mean GLP-1$^+$ cell diameter (left bars) and mean insulin$^+$ cell diameter (right bars) in neogenic pancreas (L1-L5) and mature pancreatic lobes (L6). Cell diameter was measured in confocal images after double immunostaining for insulin (green) and GLP-1 (red) in pancreatic sections from the T2DM + Lira group. For each stage, $\geq$30 cells were measured. Data were analyzed using one-way ANOVA. (C) Representative images of pancreatic sections from

(to be Continued.)

In general, these findings establish that the scattered single beta- and alpha-cells in neogenic pancreas are newborn immature cells, providing additional evidence of pancreas neogenesis following liraglutide treatment. Identities of scattered single beta- and alpha-cells in the tubuli-vesicular structure of Control and T2DM groups were also examined, and the same results were obtained (see supplementary Fig. S2).

Endocrine Progenitors and Pancreatic Stem Cells Exist in the Tubuli-Vesicular Structure

The ability of the primitive bud to give rise to both exocrine and endocrine cells implies the presence of endocrine progenitors and pancreatic stem cells.

In addition to the insulin[+]/GLP-1^{+} bihormonal cells in the tubuli-vesicular structure, we also observed single somatostatin[+] δ-cells and pancreatic polypeptide[+] PP-cells (indicated by yellow arrows; Fig. 6A). Moreover, insulin[+]/GLP-1^{+} bihormonal cells coexpressed somatostatin and PP (indicated by white arrows), indicating that they were four-hormonal cells (Fig. 6A). During embryo development, endocrine cells derived from Ngn3^{+} endocrine progenitors transiently coexpress four hormones before differentiating into monohormonal cells[32–34]. These four-hormonal cells are direct progenitors of beta-, alpha-, δ-, and PP-cells[35,36].

We probed the characteristics of four-hormonal cells. PC1/3 is a common hormone convertase that participates in posttranscriptional cleavage of proinsulin and proglucagon to generate insulin and GLP-1, respectively[37]. Consistent with their high expression of insulin and GLP-1, four-hormonal cells expressed high levels of PC1/3, relatively low levels of PC2 (Fig. 6B), and high levels of stem cell markers OCT4 and GLP-1R (indicated by white arrows; Fig. 6B). These results indicate that four-hormonal cells are pluripotent and can be directly stimulated by GLP-1 through GLP-1R.

Previous studies have demonstrated that Ngn3^{+} cells serve as endocrine progenitors during development[34,38]. Ngn3 expression was lower in the tubuli-vesicular structure than in the embryonic pancreas but clearly detectable (Fig. 6C). These results suggest that the tubuli-vesicular structure contains Ngn3^{+} endocrine progenitors and four-hormonal cells. We found the same results in Control and T2DM groups (data not shown).

The ability of the tubuli-vesicular structure to give rise to both endocrine and exocrine pancreas provides direct evidence for the existence of pancreatic stem cells. However, no generally accepted pancreatic stem cell markers are currently available. If liraglutide induces pancreas neogenesis by directly stimulating pancreatic stem cells, these cells should express GLP-1R. However, no nonhormonal GLP-1R^{+} cells were detected, indicating that the effect of liraglutide on pancreatic stem cells may be indirect. Several studies have reported that pancreatic stem cells may express Nestin, an intermediate filament protein that is a sensitive but not specific marker of neural precursor cells[39,40]. A few Nestin^{+} cells were found in the tubuli-vesicular structure, but further investigation is needed to determine whether these cells can give rise to exocrine and endocrine cells (Fig. 6D). Based on the above findings, we propose a scheme of pancreas neogenesis and the various cell types involved (Fig. 6E).

Discussion

This study demonstrates that (1) adult mice maintain the ability to regenerate pancreas from the primitive bud, and (2) liraglutide treatment facilitates intact pancreas neogenesis from the primitive bud in adult T2DM mice.

Both human and rodent pancreases have been regarded as non-regenerative organs. Although neogenesis of endocrine cells has been observed in postnatal pancreas or after partial duct ligation of adult pancreas[26,41], intact pancreas neogenesis in adult human or rodent has not been reported. In the present study, a tubuli-vesicular structure connected to pancreas was observed in healthy and metabolically altered adult mice, and liraglutide stimulated neogenesis of pancreatic lobes. To our knowledge, this is the first time such a structure has been reported, and no other data on this structure are available. Therefore, we designated it as "tubuli-vesicular structure" based on its morphological characteristics observed by light microscopy. The morphology of this structure is similar to that of loose connective tissue and adipose tissue around pancreas, and perhaps this explains why it has not been discovered previously.

The tubuli-vesicular structure appears to be pancreatic tissue in a more primitive state. It differs from mature

Figure 5. (Continued). T2DM + Lira and Control groups after immunostaining for insulin (green) and FoxO1 or NKX6.1 or PDX1 (red). Confocal images on the left show immature single beta-cells in neogenic pancreas. White arrows indicate immature beta-cells expressing FoxO1 and NKX6.1 in cytoplasm. Confocal images on the right show mature beta-cells in islets of Control mice. FoxO1 was expressed in cytoplasm of mature beta-cells (shown as yellow cells). NKX6.1 and PDX1 were expressed in nucleus of mature beta-cells (shown as purple nuclei). (D) Confocal images on the left show representative images of pancreatic sections from the T2DM + Lira group after immunostaining for GLP-1 (green) and Gcg or PC1/3 or PC2 (red). The white arrow indicates immature single alpha-cells expressing PC2. Confocal images on the right show representative images of pancreatic sections from the Control group after immunostaining for Gcg (green) and GLP-1 or PC1/3 or PC2 (red). White arrows indicate mature alpha-cells in islets of Control group expressing PC2. Significant differences: *P < 0.05. ns, no significant difference. DAPI: 4'6'-diamidino-2-phenyl-indole; FoxO1: forkhead box O1; Gcg: glucagon; GLP-1: glucagon-like peptide-1;; Lira: liraglutide; NKX6.1: NK6 homeobox transcription factor-related locus 1; PC: prohormone convertase; PDX1: pancreatic and duodenal homeobox 1; T2DM: type 2 diabetes mellitus.
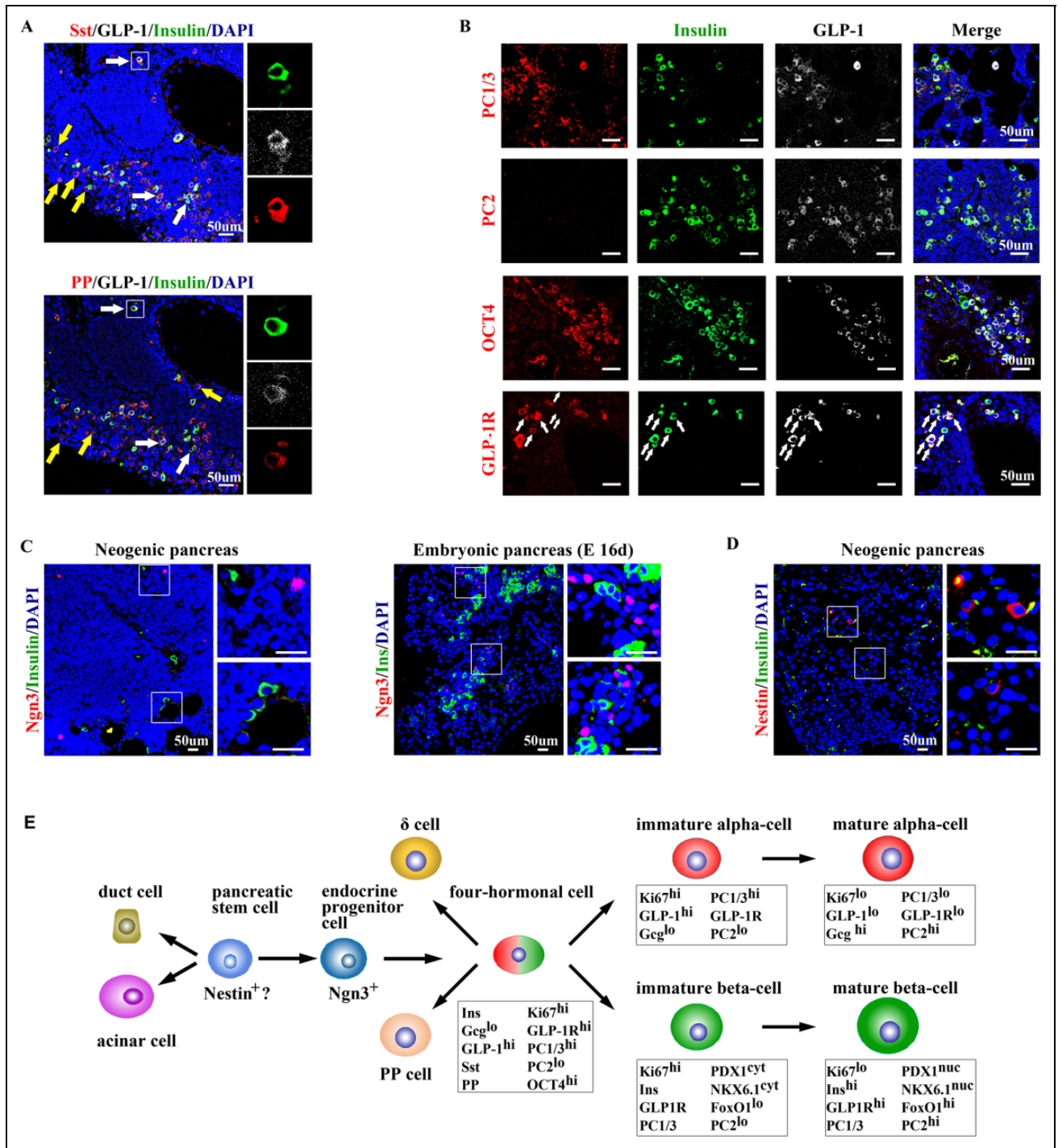
Figure 6. Endocrine progenitors and pancreatic stem cells in neogenic pancreas of T2DM + Lira mice. (A) Upper confocal images show representative images of pancreatic sections from T2DM + Lira group after immunostaining for insulin (green), GLP-1 (white), and somatostatin (red). Lower confocal images show immunofluorescence (IF) staining for insulin (green), GLP-1 (white), and pancreatic polypeptide (red) on the corresponding pancreatic section from the same mouse of T2DM + Lira group. White arrow indicates the same one insulin$^+$/GLP-1$^+$ cell in the upper and lower confocal images. The same one insulin$^+$/GLP-1$^+$ cell expressed both Sst and PP, namely insulin$^+$/GLP-1$^+$/Sst$^+$/PP$^+$ four-hormonal cells. Images on the right are enlarged views of insulin$^+$/GLP-1$^+$/Sst$^+$/PP$^+$ cells on the left. Yellow arrows indicate Sst$^+$ cells or PP$^+$ cells. (B) Representative images of pancreatic sections from T2DM + Lira group after immunostaining for insulin (green), GLP-1 (white), and PC1/3, PC2, OCT4, or GLP-1R (red). White arrows indicate insulin$^+$/GLP-1$^+$ cells coexpressing GLP-1R. (C) Representative images of pancreatic sections from the T2DM + Lira group and mouse embryo immunostaining for insulin (green) and Ngn3 (red). Images on the right are enlarged views of Ngn3$^+$ cells (cells with purple nucleus). (D) Representative images of pancreatic

(to be Continued.)

pancreatic lobes in that it has no exocrine gland and therefore no acinar cells or pancreatic ductal cells, and it contains single endocrine cells in a relatively primitive differentiation state scattered throughout, including Ngn3^{+} endocrine progenitors, incompletely differentiated four-hormonal cells, and immature alpha- or beta-cells. The scattered distribution of single endocrine cells is similar to the reported distribution in the embryonic pancreas of mice and humans[32,42], although we did not observe the exocrine cells that are present in embryonic pancreas. These differences between the tubuli-vesicular structure and the mature and embryonic pancreas suggest the identification of a unique structure in mice.

We found that 4 wk of liraglutide treatment stimulated the tubuli-vesicular structure to generate immature pancreatic lobes (L3–L5) in 22-wk-old mice. This event corresponds to pancreatic neogenesis because mice older than 4 wk do not generate new pancreatic lobes (so-called immature pancreatic lobes)[26]. We conclude that the tubuli-vesicular structure is the primitive bud that gives rise to immature pancreatic lobes. These results demonstrate that the tubuli-vesicular structure in adult mice can give rise to intact pancreas under appropriate conditions, and that the ability to regenerate is not lost during development. In fact, this capacity to give rise to intact pancreatic lobes may be the most important physiological function of the tubuli-vesicular structure in adult mice.

These findings may make sense from an evolutionary perspective; the body can preserve regenerative capacity of the pancreas into adulthood in preparation for future metabolic needs, such as pregnancy, aging, and metabolic stress. One type of metabolic stress, T2DM, did not stimulate the growth of the tubuli-vesicular structure; instead, the GLP-1 analog did. Further studies of regenerative pancreas therapy should examine the factors and mechanisms affecting the size of the tubuli-vesicular structure.

Pancreas development is a continuous process, including growth and maturation of exocrine and endocrine glands. A continuous developmental process was observed in all eight T2DM + Lira mice, consistent with reports of prenatal islet development and postnatal exocrine pancreas growth in mice during the first week after birth[26,42,43]. We were able to distinguish five stages (L1–L5) of neogenesis from the tubuli-vesicular structure into immature pancreatic lobes, based on developmental stages of embryonic pancreas in mice and humans[25,31,41,42], as well as the unique characteristics of exocrine and endocrine glands in each stage.

In our study, endocrine and exocrine glands further contributed to the development of immature pancreatic lobes (stages L3–L5). In immature pancreatic lobes, single endocrine cells were scattered throughout or aggregated into islet-like clusters of fewer than 10 cells or small islets. The proportion of incompletely differentiated insulin[+]/GLP-1^{+} bihormonal cells among all endocrine cells was much higher in immature pancreatic lobes than in mature pancreatic lobes. Mature pancreatic lobes were composed of alpha-, beta-, δ-, and PP-cells aggregated into large islets with a monohormonal insulin core in the endocrine gland. The exocrine gland in immature pancreatic lobes contained a substantial number of mesenchymal cells, which accumulated around acinar cells, giving them a loose appearance. In contrast, mature pancreatic lobe was dominated by exocrine cells. There were nearly no mesenchymal cells around acinar cells, giving the lobe a packed appearance. These characteristics of exocrine and endocrine glands make it easy to distinguish immature pancreatic lobes from mature ones.

Previous studies have reported that in mice and nonhuman primates, liraglutide treatment causes an increase in exocrine cell mass without altering the composition of endocrine and exocrine cellular compartments. In addition, proliferation rate of the exocrine tissue is low and comparable between groups[15]. These observations are consistent with our results showing that liraglutide increases pancreas mass by inducing intact pancreas neogenesis.

Intact pancreas neogenesis provides an islet microenvironment in addition to the neogenic beta-cells. Islet microenvironment greatly influences beta-cell function, survival, and proliferation[44]. Compared with islets transplantation, neogenic pancreas has better function in terms of glucose sensing and regulation. These functions are important for diabetes patients. Therefore, further investigation of the mechanisms underlying the effects of liraglutide on pancreas neogenesis may have important clinical value.

However, liraglutide treatment may increase the risk of pancreatitis or pancreatic cancer[19,20]. In the present study, both the neogenic and pre-existing pancreas showed normal histological composition and structure, excluding the possibility of pancreatic cancer development under these experimental conditions. These results are consistent with findings in mice, rats, and nonhuman primates treated with liraglutide or semaglutide, which showed no preneoplastic proliferative lesions and histopathological changes in pancreas[15,45]. Additionally, these results are consistent with observations in incretin-treated T2DM patients, who did not present marked histological abnormalities in the pancreas[46]. Future work

Figure 6. (Continued). sections from T2DM + Lira group after immunostaining for insulin (green) and Nestin (red). Images on the right are enlarged views of Nestin^{+} cells (red cells). (E) Schematic showing pancreas neogenesis and cell types involved. cyt: cytoplasm; DAPI: 4'6'-diamidino-2-phenyl-indole; FoxO1: forkhead box O1; Gcg: glucagon; GLP-1: glucagon-like peptide-1; hi: high; Ins: insulin; Lira: liraglutide; lo: low; NKX6.1: NK6 homeobox transcription factor-related locus 1; nuc: nucleus; OCT: octamer-binding transcription factor-4; PC: prohormone convertase; PDX1: pancreatic and duodenal homeobox 1; PP: pancreatic polypeptide; Sst: somatostatin; T2DM: type 2 diabetes mellitus.

should examine the possibility of liraglutide-induced pancreatitis under these conditions.

In mouse, embryonic beta-cells are described as immature, highly proliferative, and unipotent, albeit still plastic[47]. After birth, beta-cells are abundant, organized in clusters, and follow a biphasic pattern of maturation[47]. We demonstrated that scattered single alpha- and beta-cells in neogenic pancreas are newborn immature cells, based on their small size, high proliferative ability, high expression of PC1/3 and GLP-1 in single alpha-cells, and low expression of FoxO1 and NKX6.1 in single beta-cells[27,28,31,47]. These results provide additional evidence for liraglutide-induced pancreatic neogenesis. Identities of scattered single beta- and alpha-cells in the tubuli-vesicular structure of Control and T2DM groups were also examined, and the same results were obtained.

In contrast to previous studies showing that PDX1 is located in the nucleus in the developing pancreas and in adult beta-cells[48], we localized NKX6.1 and PDX1 in the cytoplasm of single beta-cells. Some studies have reported that PDX1 and NKX6.1 can shuttle between the cytoplasm and nucleus[49–51]. Future work is needed to examine whether PDX1 and NKX6.1 localize to the nucleus of single beta-cells.

We have strong evidence for liraglutide-induced intact pancreas neogenesis from the tubuli-vesicular structure (namely, the primitive bud). At the same time, the generation of hormonal cells in the neogenic pancreas appeared to differ from that in fetal pancreas under physiological conditions. It has been reported that new hormonal cells are derived from Ngn3^{+} endocrine progenitors in embryonic pancreas[34,38]. We also detected abundant Ngn3^{+} cells in mouse embryonic pancreas but relatively few Ngn3^{+} cells in neogenic pancreas. Given the high expression of GLP-1R in four-hormonal cells, these results raise the possibility that monohormonal cells in neogenic pancreas may be derived directly from four-hormonal cells and Ngn3^{+} endocrine progenitors. In addition, given the high proliferation rate of immature alpha- and beta-cells in the primitive bud and data showing that liraglutide promotes cell proliferation in vivo[8,9], monohormonal cells in neogenic pancreas may also be derived from the proliferation of pre-existing immature alpha- and beta-cells in the primitive bud.

The existence of adult pancreatic stem cells has been debated for years[52]. Given the full lineage potential of the primitive bud to give rise to both exocrine and endocrine cells, our study provides direct evidence for the existence of pancreatic stem cells, which should reside in the primitive bud. Nestin has been reported as a possible marker of pancreatic stem cells[39,40]. Nestin^{+} stem cells can be stimulated to differentiate into pancreatic endocrine and exocrine cells *in vitro*[40]. In our study, several Nestin^{+} cells were observed in the primitive bud. Whether these Nestin^{+} cells are pancreatic stem cells and whether they are regulated by GLP-1 should be investigated in future work, which should screen for stem cell makers other than Nestin.

Based on the findings of this study, we define the tubuli-vesicular structure as a primitive bud connected to pancreas, which is preserved in all adult mice and capable of generating neogenic pancreas under appropriate conditions. This structure is characterized by scattered single monohormonal cells positive for insulin, GLP-1, somatostatin, or PP; four-hormonal cells; Ngn3^{+} endocrine progenitors; and Nestin^{+} cells. It has no exocrine gland. Future studies should examine whether the primitive bud and pancreatic stem cells also exist in adult human pancreas; if so, regenerative therapy may be possible in patients with diabetes. Although GLP-1 analog is well known as an insulin secretagogue in diabetes therapy, the capacity of liraglutide to stimulate pancreas neogenesis in vivo demonstrates that GLP-1 has clinically exploitable functions other than stimulating insulin secretion in the context of diabetes.

Authors' Contributions

Hongjun Deng designed the study, performed experiments and data analysis, and wrote the manuscript. Fengying Yang, Xiaoyi Ma, Ying Wang, and Qi Chen contributed to the concept and study design. Li Yuan is the guarantor of this work, has full access to all the data in the study, and takes responsibility for the integrity of the data and the accuracy of the data analysis.

Ethical Approval

This study was approved by the Experimental Animals Committee of Huazhong University of Science and Technology, Hubei Province, China.

Statement of Human and Animal Rights

All of the experimental procedures involving animals were conducted in accordance with the Institutional Animal Care Guidelines of Huazhong University of Science and Technology, China, and were approved by the Experimental Animals Committee of Huazhong University of Science and Technology, Hubei Province, China.

Statement of Informed Consent

There are no human subjects in this article and informed consent is not applicable.

Data Availability Statement

The datasets generated during and/or analyzed during the current study are available from the corresponding author on reasonable request.

Declaration of Conflicting Interests

The author(s) declared no potential conflicts of interest with respect to the research, authorship, and/or publication of this article.

Funding

ORCID iD

Li Yuan ⓘ https://orcid.org/0000-0001-6474-746X

Supplemental Material

Supplemental material for this article is available online.

References

1. Weir GC, Gaglia J, Bonner WS. Inadequate beta-cell mass is essential for the pathogenesis of type 2 diabetes. Lancet Diabetes Endocrinol. 2020;8(3):249–256.

2. Bertin A, Sane F, Gmyr V, Lobert D, Dechaumes A, Kerr CJ, Pattou F, Hober D. Coxsackievirus-B4 infection of human primary pancreatic ductal cell cultures results in impairment of differentiation into insulin-producing cells. Viruses. 2019; 11(7):597.

3. Petrak O, Klimova J, Mraz M, Haluzikova D, Petrakova DR, Kratochvilova H, Lacinova Z, Novak K, Michalsky D, Waldauf P, Holaj R, et al. Pheochromocytoma with adrenergic biochemical phenotype shows decreased Glp-1 secretion and impaired glucose tolerance. J Clin Endocrinol Metab. 2020; 105(6):154.

4. Davis EM, Sandoval DA. Glucagon like peptide-1: actions and influence on pancreatic hormone function. Compr Physiol. 2020;10(2):577–595.

5. Quarta C, Clemmensen C, Zhu Z, Yang B, Joseph SS, Lutter D, Yi CX, Graf E, Garcia CC, Legutko B, Fischer K, et al. Molecular integration of incretin and glucocorticoid action reverses immunometabolic dysfunction and obesity. Cell Metab. 2017; 26(4):620–632.

6. O'Neil PM, Birkenfeld AL, McGowan B, Mosenzon O, Pedersen SD, Wharton S, Carson CG, Jepsen CH, Kabisch M, Wilding JPH. Efficacy and safety of semaglutide compared with liraglutide and placebo for weight loss in patients with obesity: a randomised, double-blind, placebo and active controlled, dose-ranging, phase 2 trial. Lancet. 2018;392(10148): 637–649.

7. Kannt A, Nygaard MA, Kammermeier C, Elvert R, Klockener T, Bossart M, Haack T, Evers A, Lorenz K, Hennerici W, Rocher C, et al. Incretin combination therapy for the treatment of non-alcoholic steatohepatitis (published online ahead of print,2020 Mar 20). Diabetes Obes Metab. 2020. DOI: 10.1111/dom.14035.

8. Graham GV, McCloskey A, Abdel WYH, Conlon JM, Flatt PR. A long-acting, dual-agonist analogue of lamprey GLP-1 shows potent insulinotropic, beta-cell protective, and anorexic activities and improves glucose homeostasis in high fat-fed mice. Mol Cell Endocrinol. 2020;499:110584.

9. Xu G, Stoffers DA, Habener JF, Bonner WS. Exendin-4 stimulates both beta-cell replication and neogenesis, resulting in increased beta-cell mass and improved glucose tolerance in diabetic rats. Diabetes. 1999;48(12):2270–2276.

10. Fosgerau K, Jessen L, Lind TJ, Osterlund T, Schaeffer LK, Rolsted K, Brorson M, Jelsing J, Skovlund RNT. The novel GLP-1-gastrin dual agonist, ZP3022, increases beta-cell mass and prevents diabetes in db/db mice. Diabetes Obes Metab. 2013;15(1):62–71.

11. Suarez PWL, Lakey JR, Rabinovitch A. Combination therapy with glucagon-like peptide-1 and gastrin induces beta-cell neogenesis from pancreatic duct cells in human islets transplanted in immunodeficient diabetic mice. Cell Transplant. 2008; 17(6):631–640.

12. Ansarullah Free C, Christopherson J, Chen Q, Gao J, Liu C, Naji A, Rabinovitch A, Guo Z. Activation of GPR119 stimulates human beta-cell replication and neogenesis in humanized mice with functional human islets. J Diabetes Res. 2016;2016: 1620821.

13. Sasaki S, Miyatsuka T, Matsuoka TA, Takahara M, Yamamoto Y, Yasuda T, Kaneto H, Fujitani Y, German MS, Akiyama H, Watada H, et al. Activation of GLP-1 and gastrin signalling induces in vivo reprogramming of pancreatic exocrine cells into beta cells in mice. Diabetologia. 2015;58(11):2582–2591.

14. Lee YS, Lee C, Choung JS, Jung HS, Jun HS. Glucagon-like peptide 1 increases beta-cell regeneration by promoting alpha- to beta-cell transdifferentiation. Diabetes. 2018;67(12): 2601–2614.

15. Gotfredsen CF, Molck AM, Thorup I, Nyborg NC, Salanti Z, Knudsen LB, Larsen MO. The human GLP-1 analogs liraglutide and semaglutide: absence of histopathological effects on the pancreas in nonhuman primates. Diabetes. 2014;63(7): 2486–2497.

16. Koehler JA, Baggio LL, Cao X, Abdulla T, Campbell JE, Secher T, Jelsing J, Larsen B, Drucker DJ. Glucagon-like peptide-1 receptor agonists increase pancreatic mass by induction of protein synthesis. Diabetes. 2015;64(3):1046–1056.

17. Barriere DA, Noll C, Roussy G, Lizotte F, Kessai A, Kirby K, Belleville K, Beaudet N, Longpre JM, Carpentier AC, Geraldes P, et al. Combination of high-fat/high-fructose diet and low-dose streptozotocin to model long-term type-2 diabetes complications. Sci Rep. 2018;8(1):424.

18. Abdulreda MH, Rodriguez DR, Caicedo A, Berggren PO. Liraglutide Compromises Pancreatic beta Cell Function in a Humanized Mouse Model. Cell Metab. 2016;23(3):541–546.

19. Gier B, Matveyenko AV, Kirakossian D, Dawson D, Dry SM, Butler PC. Chronic GLP-1 receptor activation by exendin-4 induces expansion of pancreatic duct glands in rats and accelerates formation of dysplastic lesions and chronic pancreatitis in the Kras(G12D) mouse model. Diabetes. 2012;61(5): 1250–1262.

20. Ryder RE. The potential risks of pancreatitis and pancreatic cancer with GLP-1-based therapies are far outweighed by the proven and potential (cardiovascular) benefits. Diabet Med. 2013;30(10):1148–1155.

21. Vetter ML, Johnsson K, Hardy E, Wang H, Iqbal N. Pancreatitis incidence in the exenatide BID, exenatide QW, and exenatide QW suspension development programs: pooled analysis of 35 clinical trials. Diabetes Ther. 2019;10(4):1249–1270.

22. Nachnani JS, Bulchandani DG, Nookala A, Herndon B, Molteni A, Pandya P, Taylor R, Quinn T, Weide L, Alba LM. Biochemical and histological effects of exendin-4 (exenatide) on the rat pancreas. Diabetologia. 2010;53(1):153–159.

23. Pothuraju R, Rachagani S, Junker WM, Chaudhary S, Saraswathi V, Kaur S, Batra SK. Pancreatic cancer associated with obesity and diabetes: an alternative approach for its targeting. J Exp Clin Cancer Res. 2018;37(1):319.

24. Butler AE, Galasso R, Matveyenko A, Rizza RA, Dry S, Butler PC. Pancreatic duct replication is increased with obesity and type 2 diabetes in humans. Diabetologia. 2010;53(1):21–26.

25. Xuan X, Gao F, Ma X, Huang C, Wang Y, Deng H, Wang S, Li W, Yuan L. Activation of ACE2/angiotensin (1-7) attenuates pancreatic beta cell dedifferentiation in a high-fat-diet mouse model. Metabolism. 2018;81:83–96.

26. Bonner WS, Aguayo MC, Weir GC. Dynamic development of the pancreas from birth to adulthood. Ups J Med Sci. 2016; 121(2):155–158.

27. Puri S, Roy N, Russ HA, Leonhardt L, French EK, Roy R, Bengtsson H, Scott DK, Stewart AF, Hebrok M. Replication confers beta cell immaturity. Nat Commun. 2018;9(1):485.

28. Bader E, Migliorini A, Gegg M, Moruzzi N, Gerdes J, Roscioni SS, Bakhti M, Brandl E, Irmler M, Beckers J, Aichler M, et al. Identification of proliferative and mature beta-cells in the islets of Langerhans. Nature. 2016;535(7612):430–434.

29. Spaeth JM, Gupte M, Perelis M, Yang YP, Cyphert H, Guo S, Liu JH, Guo M, Bass J, Magnuson MA, Wright C, et al. Defining a novel role for the Pdx1 Transcription factor in islet beta-cell maturation and proliferation during weaning. Diabetes. 2017;66(11):2830–2839.

30. Chen YC, Taylor AJ, Verchere CB. Islet prohormone processing in health and disease. Diabetes Obes Metab. 2018;20(suppl 2):64–76.

31. Habener JF, Stanojevic V. alpha-cell role in beta-cell generation and regeneration. Islets. 2012;4(3):188–198.

32. Riopel M, Li J, Fellows GF, Goodyer CG, Wang R. Ultrastructural and immunohistochemical analysis of the 8-20 week human fetal pancreas. Islets. 2014;6(4):e982949.

33. Memon B, Abdelalim EM. Stem cell therapy for diabetes: beta cells versus pancreatic progenitors. Cells. 2020;9(2):283.

34. Cai Q, Bonfanti P, Sambathkumar R, Vanuytsel K, Vanhove J, Gysemans C, Debiec RM, Raitano S, Heimberg H, Ordovas L, Verfaillie CM, et al. Prospectively isolated NGN3-expressing progenitors from human embryonic stem cells give rise to pancreatic endocrine cells. Stem Cells Transl Med. 2014;3(4): 489–499.

35. Katsuta H, Akashi T, Katsuta R, Nagaya M, Kim D, Arinobu Y, Hara M, Bonner WS, Sharma AJ, Akashi K, Weir GC. Single pancreatic beta cells co-express multiple islet hormone genes in mice. Diabetologia. 2010;53(1):128–138.

36. Teitelman G, Alpert S, Polak JM, Martinez A, Hanahan D. Precursor cells of mouse endocrine pancreas coexpress insulin, glucagon and the neuronal proteins tyrosine hydroxylase and neuropeptide Y, but not pancreatic polypeptide. Development. 1993;118(4):1031–1039.

37. Li J, Mao Z, Huang J, Xia J. PICK1 is essential for insulin production and the maintenance of glucose homeostasis. Mol Biol Cell. 2018;29(5):587–596.

38. Xu X, D'Hoker J, Stangé G, Bonné S, De Leu N, Xiao X, Van De Casteele M, Mellitzer G, Ling Z, Pipeleers D, Bouwens L, et al. β Cells can be generated from endogenous progenitors in injured adult mouse pancreas. Cell. 2008;132(2):197–207.

39. Seaberg RM, Smukler SR, Kieffer TJ, Enikolopov G, Asghar Z, Wheeler MB, Korbutt G, van der Kooy D. Clonal identification of multipotent precursors from adult mouse pancreas that generate neural and pancreatic lineages. Nat Biotechnol. 2004;22(9):1115–1124.

40. Rashed S, Gabr M, Abdel AAA, Zakaria M, Khater S, Ismail A, Fouad A, Refaie A. Differentiation potential of nestin (+) and nestin (-) cells derived from human bone marrow mesenchymal stem cells into functional insulin producing cells. Int J Mol Cell Med. 2019;8(1):1–13.

41. Lee CS, De Leon DD, Kaestner KH, Stoffers DA. Regeneration of pancreatic islets after partial pancreatectomy in mice does not involve the reactivation of neurogenin-3. Diabetes. 2006;55(2):269–272.

42. Bocian SJ, Zabel M, Wozniak W, Surdyk ZJ. Polyhormonal aspect of the endocrine cells of the human fetal pancreas. Histochem Cell Biol. 1999;112(2):147–153.

43. Chintinne M, Stange G, Denys B, In 't Veld P, Hellemans K, Pipeleers MM, Ling Z, Pipeleers D. Contribution of postnatally formed small beta cell aggregates to functional beta cell mass in adult rat pancreas. Diabetologia. 2010; 53(11):2380–2388.

44. Townsend SE, Gannon M. Extracellular matrix-associated factors play critical roles in regulating pancreatic beta-cell proliferation and survival. Endocrinology. 2019;160(8):1885–1894.

45. Nyborg NC, Molck AM, Madsen LW, Knudsen LB. The human GLP-1 analog liraglutide and the pancreas: evidence for the absence of structural pancreatic changes in three species. Diabetes. 2012;61(5):1243–1249.

46. Ueberberg S, Jutte H, Uhl W, Schmidt W, Nauck M, Montanya E, Tannapfel A, Meier J. Histological changes in endocrine and exocrine pancreatic tissue from patients exposed to incretin-based therapies. Diabetes Obes Metab. 2016;18(12): 1253–1262.

47. Salinno C, Cota P, Bastidas PA, Tarquis MM, Lickert H, Bakhti M. Beta-cell maturation and identity in health and disease. Int J Mol Sci. 2019;20(21):5417.

48. Bastidas PA, Scheibner K, Lickert H, Bakhti M. Cellular and molecular mechanisms coordinating pancreas development. Development. 2017;144(16):2873–2888.

49. Lv L, Chen H, Sun J, Lu D, Chen C, Liu D. PRMT1 promotes glucose toxicity-induced beta cell dysfunction by regulating the nucleo-cytoplasmic trafficking of PDX-1 in a FOXO1-dependent manner in INS-1 cells. Endocrine. 2015;49(3): 669–682.

50. Elrick LJ, Docherty K. Phosphorylation-dependent nucleocytoplasmic shuttling of pancreatic duodenal homeobox-1. Diabetes. 2001;50(10):2244–2252.

51. Tran R, Moraes C, Hoesli CA. Controlled clustering enhances PDX1 and NKX6.1 expression in pancreatic endoderm cells derived from pluripotent stem cells. Sci Rep. 2020;10(1):1190.

52. Jiang FX, Morahan G. Pancreatic stem cells remain unresolved. Stem Cells Dev. 2014;23(23):2803–2812.